Received: 10 September 2024 | Accepted: 27 May 2025

DOI: 10.1111/jpy.70051

RESEARCH ARTICLE

Exploring the Phaeosphere: Characterizing the microbiomes of *Phaeocystis antarctica* colonies from the coastal Southern Ocean and laboratory culture

Margaret Mars Brisbin[1,2] | **McCaela Acord**[1,3] | **Rachel Davitt**[4] | **Shavonna Bent**[1,5] | **Benjamin A. S. Van Mooy**[1] | **Eliott Flaum**[6] | **Andreas Norlin**[2] | **Jessica Turner**[7] | **Arianna Krinos**[5,8] | **Harriet Alexander**[8] | **Mak Saito**[1]

[1]Department of Marine Chemistry and Geochemistry, Woods Hole Oceanographic Institution (WHOI), Woods Hole, Massachusetts, USA

[2]University of South Florida College of Marine Science, Saint Petersburg, Florida, USA

[3]Massachusetts Maritime Academy, Buzzards Bay, Massachusetts, USA

[4]Department of Marine and Coastal Sciences, Rutgers University, New Brunswick, New Jersey, USA

[5]MIT-WHOI Joint Program in Oceanography/Applied Ocean Science and Engineering, Cambridge, Massachusetts, USA

[6]Graduate Program in Biophysics, Stanford University, Stanford, California, USA

[7]Department of Marine Sciences, University of Connecticut, Storrs, Connecticut, USA

[8]Department of Biology, Woods Hole Oceanographic Institution, Woods Hole, Massachusetts, USA

Correspondence
Margaret Mars Brisbin, University of South Florida College of Marine Science, Sainte Petersburg, FL, USA.
Email: mmarsbrisbin@usf.edu

Funding information
Simons Foundation, Grant/Award Number: 874439; National Science Foundation, Grant/Award Number: OPP-2224611

Editor: B. Palenik

Abstract

Interactions between phytoplankton and bacteria play critical roles in shaping marine ecosystems. However, the intricate relationships within these communities—particularly in rapidly changing polar environments—remain poorly understood. We use targeted methods to directly characterize the microbiomes of individual colonies of *Phaeocystis antarctica*, a keystone phytoplankton species in the Southern Ocean, and showed that colony microbiomes were consistent across individual colonies collected 108 nautical miles apart. These results suggest that hosting specific colony microbiomes is a shared trait across colony-forming *Phaeocystis* species, with different species hosting colony microbiomes suited to their respective environments. The bacterial orders Alteromonadales, Oceanospirillales, and Sphingomonadales dominated the microbiomes of all field-collected *P. antarctica* colonies. The relative abundances of bacterial taxa comprising the majority of field-collected colony microbiomes—for example, *Paraglaciecola* sp. (Alteromonadales) and Nitrincolaceae (Oceanospirillales)—correlated with *Phaeocystis* abundance in surface waters, highlighting their potential roles in bloom dynamics and carbon cycling. After a year of laboratory culture, we observed a reduction in colony microbiome diversity, and Caulobacterales, Cellvibrionales, and Rhodobacterales dominated the cultured colony microbiomes. Notably, abundant genera in field-collected colony microbiomes that were lost in culture were psychrophiles. The shift in microbiome structure emphasizes the importance of field-based studies to capture the complexity of microbial interactions, especially for species from polar environments that are difficult to replicate in laboratory conditions. This research provides valuable insights into the ecological significance of prokaryotic interactions with a key phytoplankton species and underscores the necessity of considering these dynamics in the context of climate-driven shifts in marine ecosystems.

KEYWORDS
Phaeocystis antarctica, Phycosphere, phytoplankton–bacteria interactions, polar microbial ecology, southern ocean

Abbreviations: ASV, amplicon sequence variant; cDNA, complementary DNA; CTD, conductivity temperature depth; DMS, dimethyl sulfide; DMSP, dimethylsulfoniopropionate; PAL LTER, Palmer Long Term Ecological Research; PCoA, principal coordinate analysis; PCR, polymerase chain reaction; PERMANOVA, permutational analysis of variance; rRNA, ribosomal RNA; Si, silicate; SparCC, sparse correlations for compositional data; WAP, West Antarctic Peninsula.

INTRODUCTION

Interactions between phytoplankton and bacteria form the basis of sophisticated and specialized relationships that influence large-scale ecosystem processes, such as primary production, nutrient cycling, and carbon export (Seymour et al., 2017). Primary production in the coastal Southern Ocean is impacted by the interactions between bacteria with key roles in ecosystem function (Kim et al., 2022) and specific phytoplankton groups (e.g., diatoms in the genera *Fragilariopsis* and *Pseudo-nitzschia*; Bertrand et al., 2015). The coastal Southern Ocean along the West Antarctic Peninsula (WAP) is an exceptionally productive ecosystem with productivity driven by high-biomass phytoplankton blooms in the Austral spring and summer (Arrigo et al., 1998). The haptophyte alga *Phaeocystis antarctica* is a dominant early contributor to spring phytoplankton blooms and has a unique multi-morphic life history with implications for how carbon moves through the food web (DiTullio et al., 2000). *Phaeocystis antarctica* has a free-living flagellate stage and a colonial stage, in which thousands of cells coexist in a self-secreted, spherical mucilaginous colony (Schoemann et al., 2005). The colonial stage is dominant during *Phaeocystis* blooms (Smith & Trimborn, 2024), is avoided by zooplankton grazers (Ryderheim et al., 2022), and contributes to organic carbon export through sinking (DiTullio et al., 2000; Nissen & Vogt, 2021; Smith et al., 2021). The colony structure provides a unique interface for bacterial interactions that could contribute to *P. antarctica*'s ecological success. Although *P. antarctica* blooms have been shown to alter the bacterial community in the water column (Delmont et al., 2014), the *P. antarctica* colony microbiome has not been directly investigated.

Evidence from other species suggests integral roles for the microbiome of *Phaeocystis* colonies. For example, the colonies of a closely related *Phaeocystis* species (*P. globosa*) host highly specific bacterial communities that can relieve B-vitamin limitation (Mars Brisbin et al., 2022). Bacteria isolated from the surface of the Southern Ocean diatom *Pseudo-nitzschia subcurvata* included a vitamin-B_{12} synthesizing *Sulfitobacter* sp. (Rhodobacterales) that boosted the *Ps. subcurvata* growth rate and rescued it from B_{12} limitation (Andrew et al., 2022). Other bacteria isolated from *Ps. subcurvata* did not affect growth rate but extended survival in the stationary phase (Andrew et al., 2022). Earth system modeling predicts that particle-attached bacteria—like those associated with *Phaeocystis* colonies and other phytoplankton—will become more abundant in the Southern Ocean despite bacterial biomass in the oceans decreasing globally as mean sea surface temperature increases (Kim et al., 2023). These results highlight the relevance of particle and phytoplankton-associated bacteria under future climate scenarios, especially in the Southern Ocean (Kim et al., 2023). As the WAP is experiencing faster-than-average climate change (Schofield et al., 2010) and temperature-related shifts in phytoplankton communities (Schofield et al., 2017), fully characterizing interactions that could influence the abundance, productivity, and fate of keystone phytoplankton species such as *P. antarctica* is paramount.

The environmental conditions that organisms experience in the field are not perfectly emulated in laboratories in general, but this is especially so in more extreme environments like the coastal Southern Ocean, where sea surface temperatures are lower than can be maintained by typical algal incubators and sea ice is an important physical feature. Thus, culture biases (the selection for or against certain organisms) in microbiome composition may be especially pronounced for organisms isolated from relatively extreme environments. The direct and immediate assessment of microbiome composition from field-derived isolates may better portray the bacterial community that exists in situ rather than studying the microbiomes of cultured isolates, but field microbiomes are often infeasible to analyze due to limited field access or challenges in identifying and isolating small phytoplankton cells at sea. Consequently, many studies characterizing phytoplankton-associated bacteria have relied on accessible and easily manipulated cultured phytoplankton strains (Kuhlisch et al., 2024; Martínez-Pérez et al., 2024). However, the abundant large colonies comprising high-biomass *Phaeocystis antarctica* blooms (Schoemann et al., 2005) enable direct and immediate microbiome assessment. Here, we isolated *P. antarctica* colonies from the surface of the Southern Ocean and immediately processed them for microbiome analysis. These microbiomes thus contained bacterial communities physically associated with *P. antarctica* colonies in natural bloom conditions. This approach is novel compared to previous studies that have used co-occurrence in bulk samples to identify bacteria associated with *Phaeocystis* (Delmont et al., 2014) or have evaluated individual-colony microbiomes in cultured strains (Mars Brisbin et al., 2022). Identifying the bacteria physically associated with *P. antarctica* colonies allows associations between *Phaeocystis* and bacteria to be authentically assessed in bulk samples. Using higher-resolution environmental samples in space and time in conjunction with direct and immediate validation of bacterial microbiome constituents can then enable identification of taxa and interpretation of which bacterial taxa have key roles in *Phaeocystis* blooms from formation to termination.

MATERIALS AND METHODS

Study site

Sampling was performed aboard the R/V *Nathanial B. Palmer* as part of the Palmer Long Term Ecological

Research (PAL LTER) program's annual cruise along the WAP completed from November 22 to December 17 during the Austral spring of 2021. The PAL LTER annual cruise samples a grid of stations, with the primary grid lines roughly perpendicular to the coast and the secondary grid lines approximately parallel to the coast (Figure 1). Grid line numbers represent the distance in km from a point on the southern coast of the WAP (Brown et al., 2019), and station names represent the primary grid line number and the secondary grid line number separated by a period (e.g., "600.400"). The PAL LTER annual cruise usually occurs in January; thus, the spring timing of the 2021 cruise yielded a relatively unique dataset. Specifically, the 2021 cruise encountered a strong spring bloom in the continental slope region that extended offshore (Figure 1). During transit, surface water was continuously sampled through the underway system and chlorophyll *a* was monitored by a WET Lab ECO-FL Fluorometer, revealing especially high chlorophyll *a* at offshore stations along the shelf slope and corroborating satellite-based chlorophyll *a* estimates (Figure 1).

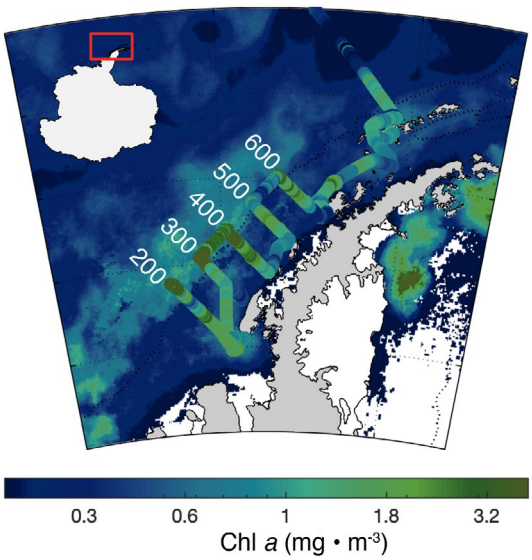

FIGURE 1 Chlorophyll *a* concentration in surface seawater near the West Antarctic Peninsula during the sampling campaign. Satellite sea-surface chlorophyll *a* was determined from CMEMS GlobColour Level-3 with the mean values from November 22 to December 17, 2021, displayed (Garnesson et al., 2019). Underway chlorophyll *a* measurements are overlaid on the satellite data using the same color scale. The study region is indicated with a red box on the inset map of Antarctica. A large offshore phytoplankton bloom is visible in the satellite data and corroborated by the underway measurements taken at the seaward ends of the Palmer Long Term Ecological Research program (PAL LTER) grid lines (labeled 200, 300, 400, 500, and 600 in white on the figure). Yellow points at the seaward ends of the 400 and 600 lines are stations 400.200 and 600.200, respectively, where *Phaeocystis antarctica* colonies were collected for microbiome analysis.

Seawater sampling for community analyses

To evaluate the influence of spring bloom phytoplankton community composition—and particularly *Phaeocystis antarctica* abundance—on bacterial communities in WAP surface waters, we performed whole-community 16S rRNA gene metabarcoding (cDNA). Two liters of surface water collected by Niskin bottle at five PAL LTER grid stations (stations 600.100, 600.200, 500.200, 400.200, and 400.100) were filtered through 47-mm diameter 0.2-μm-pore-size filters. To increase the spatial resolution of sampling, seawater from the ship's underway system was also filtered during selected transects between grid stations. Seawater from the underway system was screened through 51-μm mesh and filtered on 3.0-μm-pore-size 142-mm diameter filters using positive pressure for 1 h at a time. The GPS coordinates when filtering began and ended for each underway sample were recorded (samples integrated 3–23 nautical miles, mean = 10.25 nautical miles), along with the volume of water filtered (5.3–18 L, mean = 11 L). The 51-μm prefilter was applied to prevent zooplankton from swamping the sequencing reads in the higher-volume samples. Although the prefilter could prevent the collection of some larger phytoplankton, including *P. antarctica* colonies, many *P. antarctica* colonies have diameters less than 51 μm, and larger colonies likely passed through this prefilter due to their fluid nature. All filters were flash-frozen in liquid nitrogen, stored at −80°C on board, and transferred to coolers with dry ice for shipping to the lab.

Nucleic acid extraction and amplicon sequencing from filters

RNA was extracted from the 0.2-μm-pore-size filters (Niskin samples from PAL LTER grid stations) and one-quarter sections of the 3.0-μm-pore-size filters (underway samples) using the Qiagen RNeasy Mini Kit with additional heat and mechanical cell lysis steps. Specifically, filters and filter fractions were transferred to Zymo Scientific Bashing Bead (0.1- and 0.5-mm diameter) bead tubes with 650 μL of Qiagen RLT + βME lysis buffer; bead tubes were incubated at 65°C for 10 min before being affixed to a horizontal vortex adapter and vortexed at maximum speed on a Vortex Genie 2 for 5 min. Following the heat and mechanical lysis steps, extractions followed the manufacturer's protocol without any further modifications. RNA was extracted from filter samples to target the active portion of the microbial communities as much as possible. Extracted RNA concentration and quality were evaluated with the Qubit High Sensitivity RNA Assay and the BioAnalyzer RNA 6000 Pico Kit, respectively. RNA was reverse transcribed to cDNA using the Applied Biosystems High-Capacity RNA-to-cDNA kit before

proceeding with polymerase chain reactions (PCRs) to amplify the V3–V4 region of 16S rRNA gene. 16S rRNA PCR followed the protocol described in Illumina's "16S Metagenomic Sequencing Library Preparation" protocol with no modifications. The primers described in the Illumina protocol were used in PCRs (Forward primer: 5′ TCGTCGGCAGCGTCAGATGTGTATAAGAGACAGC CTACGGGNGGCWGCAG, Reverse primer: 5′ GTCT CGTGGGCTCGGAGATGTGTATAAGAGACAGGAC TACHVGGGTATCTAATCC; Klindworth et al., 2013) The resulting amplicons were sequenced with 300×300-bp v3 paired-end chemistry on the Illumina MiSeq Platform.

Phaeocystis colony preparation for single-colony microbiome analysis

To more directly assess the microbial communities associated with *Phaeocystis antarctica* colonies, individual colonies were isolated for 16S rRNA gene sequencing. At high-chlorophyll stations 400.200 and 600.200 (Figure 1; ~108 nautical miles apart), surface seawater water was collected into glass plankton jars from the bottom of Niskin bottles, allowing for *P. antarctica* colonies to be non-destructively sampled by preventing colony breakage from passing through the Niskin spout. Colonies in glass jars were targeted by eye, transferred to Petri dishes by large-bore pipette, and observed by light microscopy to isolate intact colonies of similar size (diameters 86–161 μm, mean = 125 μm; Figure S1). Individual colonies were rinsed three times by serially transferring the colony with minimal seawater carry-over into 200 μL of 0.2-μm-filtered seawater by large-bore pipette. After three serial rinses, the colonies were each transferred to an Axygen Maxymum Recovery 0.5-mL PCR tube with <10 μL of filtered seawater carried over. For DNA extraction, 30 μL of a 10% mass-to-volume Chelex 100 resin bead slurry in PCR-grade water was added to each PCR tube containing a single colony. Tubes containing a colony and Chelex beads were vortexed for 10 s, heated to 96°C for 20 min, vortexed again for 10 s, centrifuged briefly, and transferred to ice. The PCRs amplifying the V3–V4 region of the 16S rRNA gene were immediately performed with 10 μL of supernatant from Chelex extractions using the Bento Lab Portable PCR Workstation. The PCR conditions followed Illumina's "16S Metagenomic Sequencing Library Preparation" protocol with no modifications (using the same primers as described above). Success of the PCR was checked by gel electrophoresis, and successful reaction products were stored at −20°C before being hand-carried on ice back to the lab. Amplicons from field-collected colony microbiomes were sequenced with 300×300-bp v3 paired-end chemistry on the Illumina MiSeq Platform (Klindworth et al., 2013).

To assess the effect of culture conditions on the *Phaeocystis antarctica* colony microbiome composition, a unialgal culture was established by isolating a single colony from PAL LTER grid station 400.200, rinsing it three times with sterile seawater, and transferring it to 35 mL of L1–Si media prepared with 0.2-μm-filtered seawater (Guillard & Hargraves, 1993) in a 50-mL plastic culture flask. At sea, the culture was maintained in a Percival low-temperature algal growth chamber with LED lighting, set to mimic ambient light and temperature conditions (−1°C, 18:6 h light:dark cycle). The culture was hand-carried on ice back to the lab, where it was transferred to a walk-in cold chamber set to 4°C with 24-h light from cool white, fluorescent bulbs (recorded temperature range: 4–8°C). The culture was maintained in 100 mL of media (L1–Si in artificial seawater with a salinity of 34 prepared from Instant Ocean) in a plastic culture flask with 75% of the media replaced approximately once a month. After about a year of maintenance (in January 2023), individual colonies ($n = 14$) were isolated from the culture and processed for single-colony microbiome analysis following the same methods as the field-isolated colonies described above, except colony rinses were performed with sterile (autoclaved and 0.2-μm-filtered) artificial seawater with a salinity of 34 prepared with Instant Ocean. Amplicons from cultured colony microbiomes were sequenced with 300×300-bp v3 paired-end chemistry on the Illumina MiSeq Platform (Klindworth et al., 2013).

Sequence processing and bioinformatic analysis

Illumina sequencing for this project was completed across two flow cells processed 1 year apart but at the same sequencing facility and following the same methods. Sequences from the two sequencing runs were processed separately with the DADA2 denoising algorithm (Callahan et al., 2016) within the QIIME 2 framework (Bolyen et al., 2019), which performs quality filtering, chimera and singleton removal, and amplicon sequence variant (ASV) identification. Following denoising, the results from the two runs were merged, and the ASVs were clustered at 99% identity. Taxonomy was assigned to all representative sequences using a naive Bayes classifier trained on the SILVA 99% 16S sequence database (v138; Quast et al., 2013) using the QIIME 2 feature-classifier plug-in (Bokulich et al., 2018). Sequences classified as chloroplasts with the SILVA classifier were transferred to a new fasta file and reclassified with a naive Bayes classifier trained on the PhytoREF database (Decelle et al., 2015). Further analysis was completed in the R statistical environment (R Core Team, 2018) using the packages phyloseq (v1.34; McMurdie & Holmes, 2013), CoDaSeq (v0.99.6; Gloor et al., 2017), and vegan (v2.5–7; Oksanen et al., 2025).

RESULTS

Sequencing results

This project generated 10,368,583 paired-end sequences with 65,073–326,393 sequences per sample (mean = 326,393; Table S1). Following quality filtering, 6,768,259 sequences remained with 39,941–210,027 per sample (mean = 118,741). A total of 6,666,170 sequences were denoised (39,786–202,664 per sample, mean = 116,951), with paired-end reads for 6,371,386 denoised sequences merging (29,346–183,750 per sample, mean = 111,779) and 4,895,010 found non-chimeric (36,712–143,851 per sample, mean = 85,877). Across all samples, 14%–96% of sequences were classified as chloroplast sequences (Figure S2), with the percentage of chloroplast sequences higher among field-isolated colonies (53%–96%, mean = 76%) and cultured colonies (58%–76%) than in seawater samples. Sequences from underway samples were 44%–75% chloroplast (mean = 58%), while sequences from Niskin samples were 14%–51% chloroplast (mean = 37%). Rarefaction curves reached saturation for bacterial and chloroplast sequences in all samples (Figure S3). The bacterial ASV richness (number of unique 99% identity-clustered ASVs) was 140–317 (mean = 211) in seawater samples from the underway system and 142–209 (mean = 170) in seawater samples from Niskin bottles. The ASV richness was slightly higher in the samples collected closest to shore (Figure S4). The Shannon index for bacterial sequences in underway samples was 2.8–3.9 (mean = 3.3) and in Niskin samples was 2.3–3.2 (mean = 2.8; Figure S4). For chloroplast sequences, the ASV richness was 51–105 (mean = 79) in underway samples and 51–74 (mean = 63) in Niskin samples (Figure S5). Underway transects showed higher richness closer to shore and lower richness approaching the shelf break. Chloroplast Shannon indices were 2.1–2.7 (mean = 2.5) in underway samples and 1.9–2.7 (mean = 2.4) in underway samples, with Shannon indices also being generally lower inshore than offshore (Figure S5). Principal coordinate analyses (PCoAs) based on the Aitchison distances between chloroplast and bacterial 16S rRNA gene sequences demonstrated separation between more inshore and offshore samples along the primary axis regardless of sample type (CTD/Niskin or underway; Figure 2). However, these groupings were not found to be statistically significant (adonis2, PERMANOVA; 999 permutations, $R^2 = 0.05$, $F = 0.8$, $p = 0.52$).

Spatial variation in phytoplankton and bacterial community compositions

A clear geographical pattern in *Phaeocystis antarctica* relative abundance was apparent in the chloroplast 16S rRNA gene sequences from filtered seawater samples (>0.2-μm Niskin samples and 3.0–51 μm underway samples; Figure 3). The abundance of *Phaeocystis* relative to other phytoplankton groups increased from the more inshore mid-shelf to the more offshore stations at the shelf break, with ~50% of chloroplast 16S rRNA gene sequences belonging to *Phaeocystis* along the shelf break (Figure 3a,b). Samples collected closer to shore included larger proportions of prasinophytes and silicoflagellates (families: Prasinophyceae and Dictyochophyceae; Figure 3a,b). Cryptophytes were only detected closer to shore and between stations 600.200 and 500.200 (Figure 3a,b), where there were lower chlorophyll *a* concentrations in the surface waters (Figure 1), but cryptophyte relative abundance remained low even where they were detected. The bacterioplankton community showed a similar geographic pattern, with communities shifting from higher diversity closer to shore to lower diversity at the shelf break

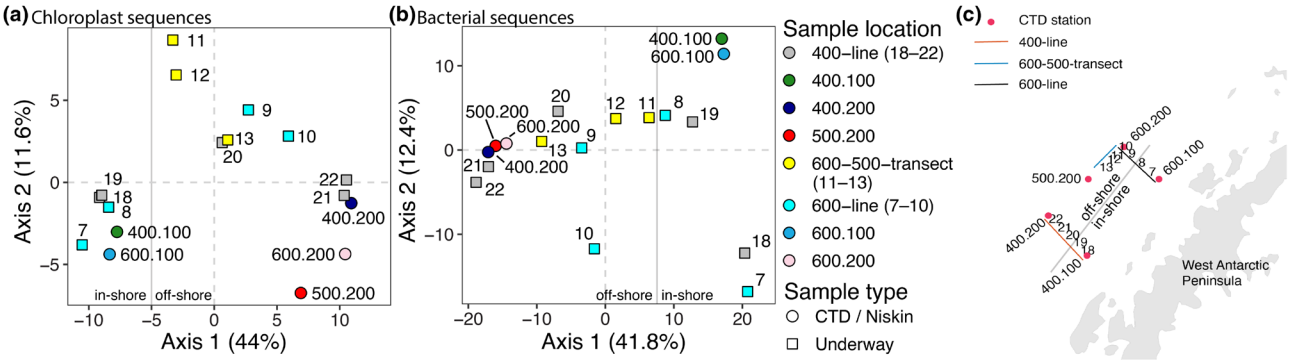

FIGURE 2 Principal coordinate analysis results based on the Aitchison distances between chloroplast (a) and bacterial (b) 16S rRNA gene sequences in seawater samples collected from Niskin bottles and from the ship's underway seawater sampling system. Samples separated along the primary axis by sampling location for both chloroplast (a) and bacterial (b) 16S rRNA gene sequences. Specifically, inshore and offshore samples separated along the primary axis, and this is notated on panels a–c by a solid gray line with inshore and offshore sides labeled. Panel c is a geographic legend for sample locations included in panels a and b. Inshore and offshore groupings were not statistically significant by PERMANOVA (adonis2, 999 permutations, $p > 0.05$).

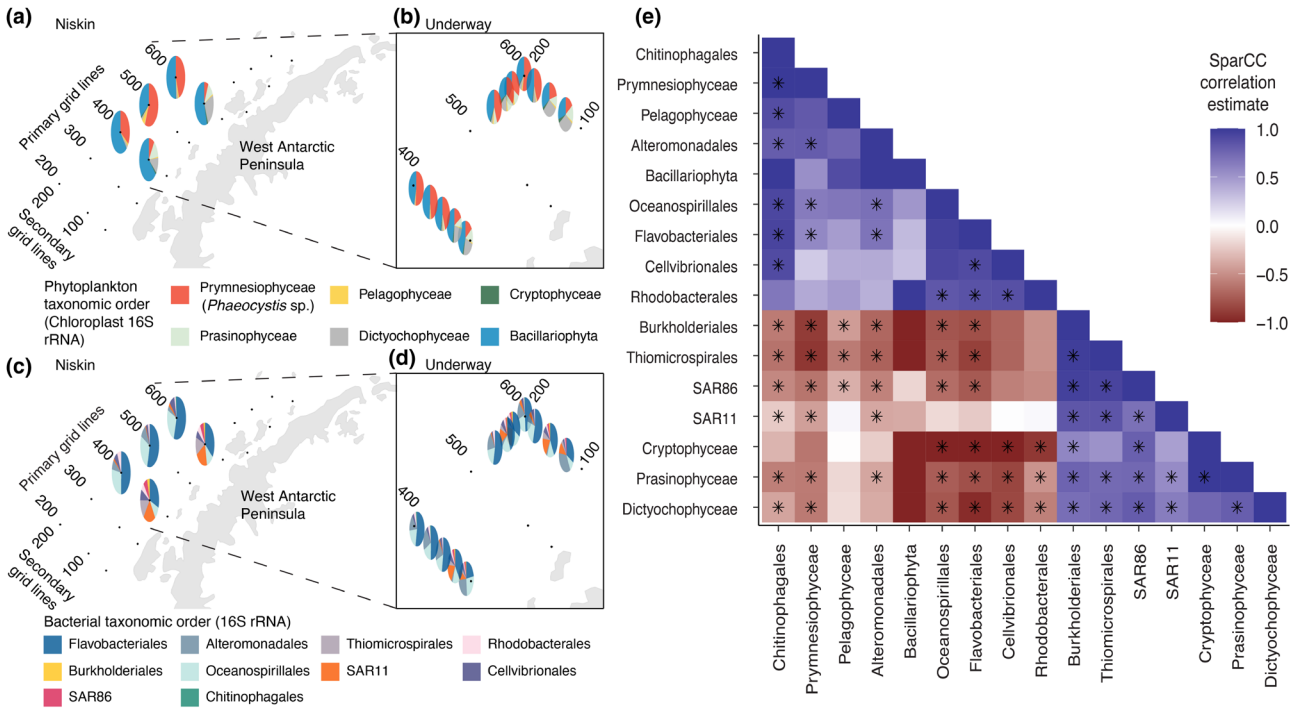

FIGURE 3 Relative abundances of major phytoplankton (a, b) and bacterial (c, d) taxonomic orders in seawater samples collected along the western Antarctic Peninsula and the correlation between major groups in seawater samples (e). (a, b) Relative abundances of major phytoplankton orders in Niskin and underway samples based on chloroplast 16S rRNA gene sequences are denoted by pie charts arranged to match the geographic location where the samples were collected. Numbers at the ends of gridlines perpendicular to the peninsula (200, 300, 400, 500, 600) denote the primary gridlines, whereas numbers at the ends of gridlines roughly parallel to the peninsula (100, 200) represent secondary gridlines. Station names were formed by combining the primary and secondary grid lines that cross at the station (e.g., 600.200). Palmer LTER grid stations are represented by black points and the grid lines are labeled. Data were plotted with the R packages ggspatial and scatterpie. (c, d) Relative abundance of major bacterial orders in Niskin and underway samples based on 16S rRNA gene sequences. (e) SparCC correlation between major phytoplankton and bacterial groups located in the western Antarctic Peninsula region. The correlation matrix is displayed as a heatmap with darker blues indicating more positively correlated groups and darker reds indicating more negatively correlated groups. 1000 bootstrap simulations were performed to calculate false discovery rate (FDR) adjusted *p*-values, and asterisks (*) on the plot indicate correlations with FDR adj. *p*-values < 0.05.

(Figure 3c,d). Flavobacteriales were more abundant at the shelf break and at stations with higher *Phaeocystis* abundance, whereas SAR11 was more abundant closer to shore and at stations with lower *Phaeocystis* abundance.

To further assess the relationship between major phytoplankton and bacterial groups in the PAL LTER region, the SparCC (sparse correlations for compositional data) method for inferring correlations was applied with 1000 bootstrap simulations to calculate false discovery rate adjusted *p*-values (Friedman & Alm, 2012). The SparCC correlation results matrix showed two modules of co-varying taxa—a module including the phytoplankton groups Prymnesiophyceae, Bacillariophyta, and Pelagophytceae and the bacterial groups Alteromonadales, Cellvibrionales, Chitinophagales, Flavobacteriales, Oceanospirillales, and Rhodobacterales and a second module containing the phytoplankton groups Cryptophyceae, Prasinophyceae, and Dictyochophyceae and the bacterial groups Burkholderiales, SAR86, SAR11, and Thiomicrospirales (Figure 3e). Prymnesiophyceae (made up of Phaeocystales ASVs) was significantly positively correlated (p-adj < 0.05) with Flavobacteriales, Oceanospirillales, Alteromonadales, and Chitinophagales and was significantly negatively correlated with Dictyochophyceae, Prasinophyceae, SAR11, SAR86, Thiomicrospirales, and Burkholderiales (Figure 3e). These results demonstrate that there are distinct communities in the mid-shelf and shelf break along the and that specific bacterial groups covary with *Phaeocystis* (Prymnesiophyceae) and other phytoplankton.

Composition of single-colony microbiomes

Collectively, the individual colonies collected from PAL LTER stations hosted two-hundred and forty-one 99% identity-clustered bacterial ASVs in their microbiomes, with 28–67 detected per colony (mean = 44, n = 26; Figure 4a). Cultured colony microbiomes were less diverse, with seventy-four 99% identity-clustered bacterial ASVs detected across all cultured colony microbiomes and 18–31 detected per colony

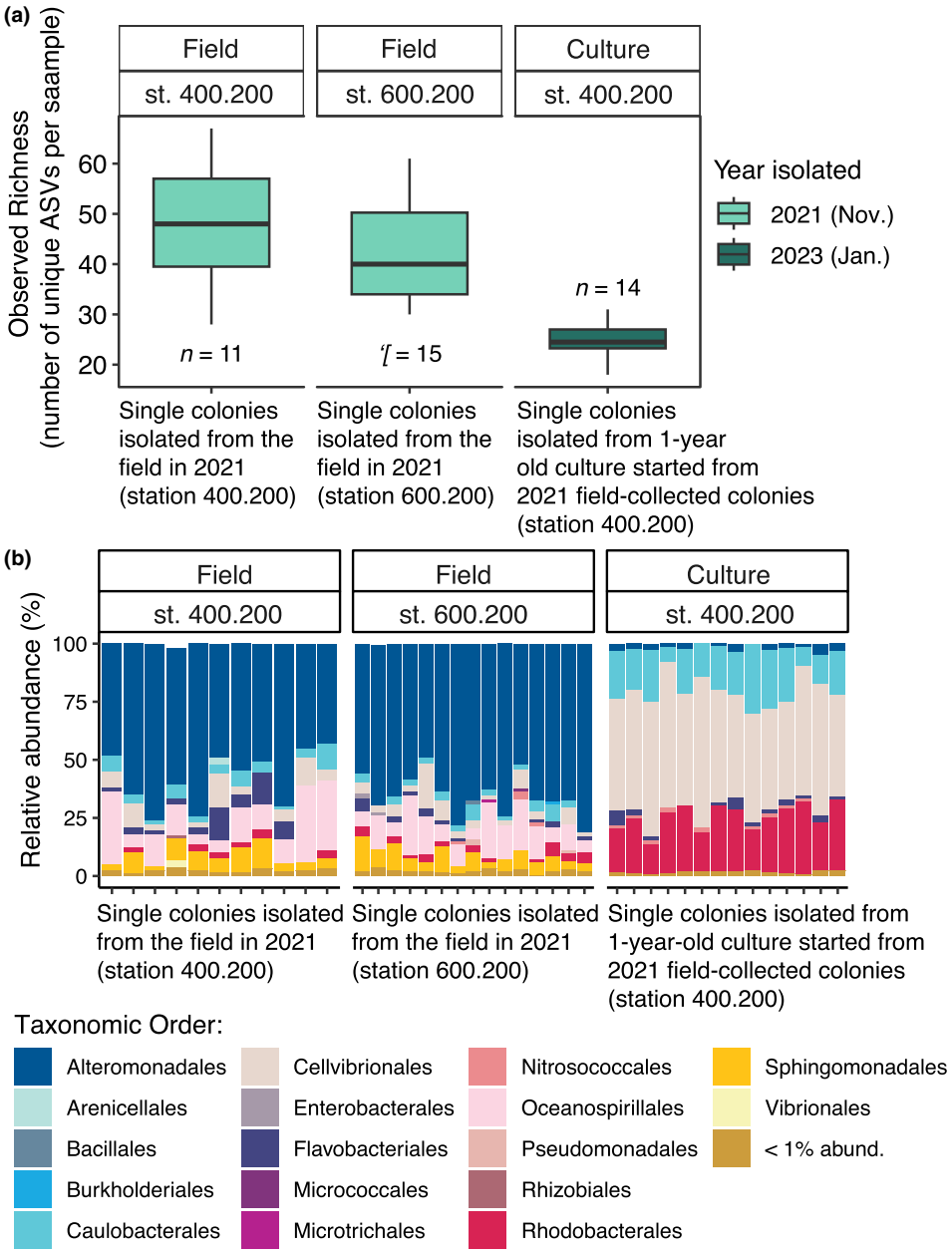

FIGURE 4 Alpha diversity and community composition of bacterial communities associated with single *Phaeocystis antarctica* colonies isolated directly from the field or after a year in culture. (a) The observed richness (i.e., number of unique 99% identity-clustered amplicon sequence variants) in each colony microbiome. The solid back lines inside boxes represent the median, boxes represent the interquartile range between the 1st and 3rd quartiles, and whiskers denote the range. Sample size (*n*) is indicated above or below each box and represents the number of individual colonies analyzed. (b) Relative abundance of bacterial orders in each colony microbiome (each column represents a single colony).

(mean = 25, $n = 14$; Figure 4a). Microbiome community compositions were consistent among field-collected colonies as well as among cultured colonies but were significantly different between field-collected and cultured colonies (adonis2, PERMANOVA, 999 permutations; $F = 44.209$, $R^2 = 0.54$, $p = 0.001$; Figure 4b, Figure S6). Alteromonadales was the most abundant bacterial order in the field-collected colony microbiomes (Figure 4b), with the majority of Alteromonadales ASVs belonging to the genera *Paraglaciecola* and *Colwellia* (Figure 5). Notably, a single *Paraglaciecola* sp. ASV comprised a large proportion of almost all field-collected colony microbiomes (mean = 32%, *SD* = 13%, range = 11%–57%, when excluding one sample with only 1% of this ASV) and was absent in all cultured colony microbiomes (Figure S7). Oceanospirillales and Sphingomonadales also comprised large proportions of most field-collected colony microbiomes (Figure 4b). In contrast, the orders Caulobacteriales, Cellvibrionales, and Rhodobacterales made up the majority of the cultured colony microbiomes (Figure 4b). A single

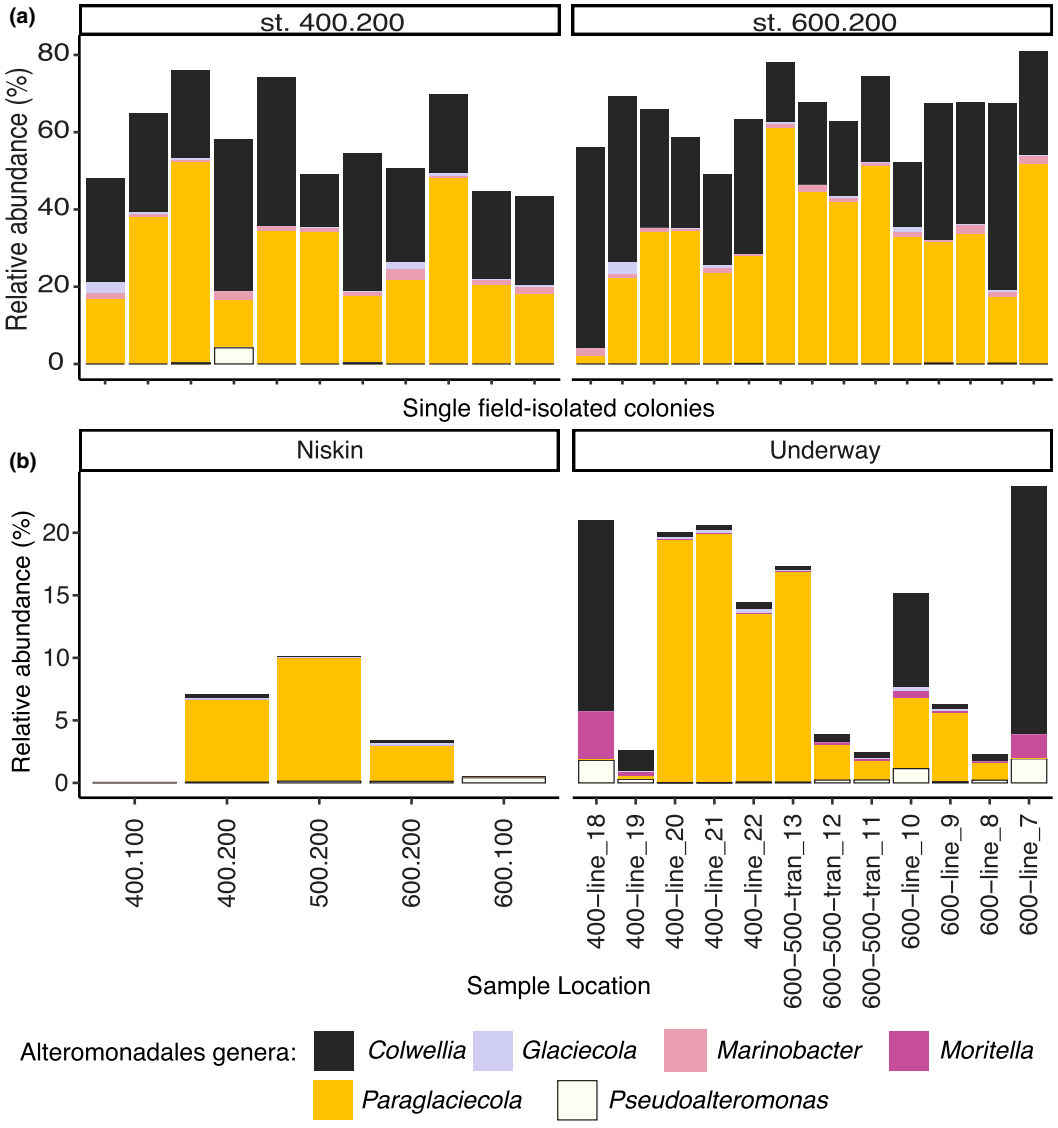

FIGURE 5 Relative abundance of Alteromonadales genera in field-collected colony microbiomes and in seawater samples. (a) The relative abundance of Alteromonadales genera in field-collected colony microbiomes is represented by a stacked bar for each individual colony. Colony microbiomes are separated into two facets labeled with the PAL LTER grid station where the colonies were isolated from. (b) The relative abundance of Alteromonadales genera detected in field-collected colonies in the seawater samples collected from the PAL LTER grid represented by a stacked bar for each sample. The plot is facetted to separate samples collected by Niskin bottles or the underway system. CTD stations and underway sample locations correspond to the notations on Figure 2c.

Sulfitobacter ASV (Rhodobacterales) that was relatively rare in field-collected colony microbiomes (range = 0%–1%, mean = 0.2%, *SD* = 0.3%) made up 12.2%–30.8% (mean = 22.1%, *SD* = 5.7%) of cultured colony microbiomes (Figure S8). Overall, the cultured colony microbiomes had reduced diversity (ASV richness) and lost most *Paraglaciecola* and all *Colwellia* (Alteromonadales), Oceanospirillales (family: Nitrincolaceae), and Sphingomonadales (family: Erythrobacteraceae) members.

Due to the high relative abundance of Alteromonadales and Oceanospirillales in field-collected colony microbiomes, these orders were investigated at higher taxonomic resolution in both field-collected colony microbiomes and in seawater samples (Figures 5 and 6). The most abundant Alteromonadales genera in both field-collected colonies and seawater samples were *Paraglaciecola* and *Colwellia*, although *Colwellia* was enriched in colony microbiomes compared to its availability in the surrounding seawater (Figure 5). In seawater samples, *Colwellia* relative abundance was highest at the most inshore sampling locations (CTD stations 400.100 and 600.100, and Underway samples 7 and 18) where *Paraglaciecola* was not detected (Figure 5). The family Nitrincolaceae made up the majority of Oceanospirillales in both field-collected colony microbiomes and in seawater samples (Figure 6). Notably, the Oceanospirillales family Alcanivoraceae was only detected in colony microbiomes and not in seawater samples. The majority of Oceanospirillales detected

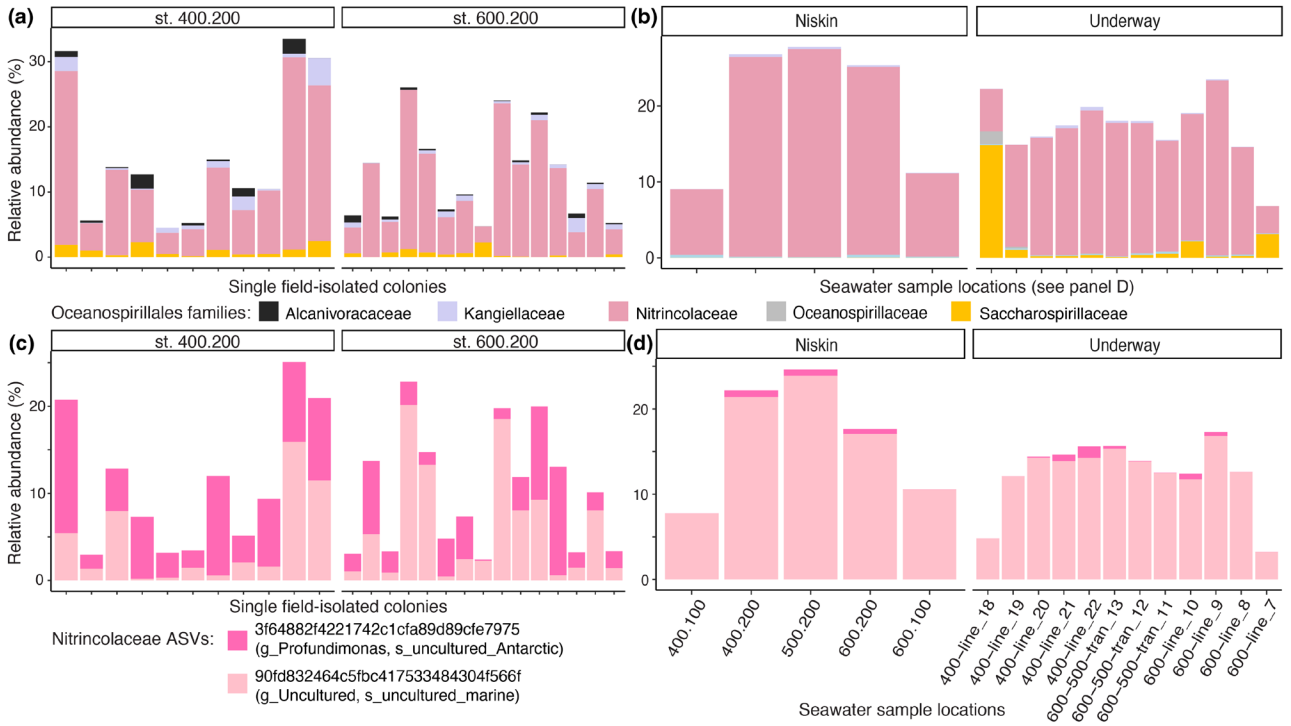

FIGURE 6 Relative abundance of Oceanospirillales families and ASVs in field-collected colony microbiomes and in seawater samples. (a) The relative abundance of Oceanospirillales families in field-collected colony microbiomes is represented by a stacked bar plot for each individual colony. Colony microbiomes are separated into two facets labeled with the PAL LTER grid station where the colonies were isolated from. (b) The relative abundance of Oceanospirillales families in seawater samples collected by Niskin or Underway from the PAL LTER grid is represented by stacked bars. The plot is facetted to separate samples collected by Niskin bottles or the underway system. CTD stations and underway sample locations correspond to the notations on Figure 2c. (c) The relative abundance of Nitrincolaceae amplicon sequence variants (ASVs) represented as stacked bar plots for each individual field-collected colony microbiome, faceted for grid station of origin. (d) The relative abundance of the same ASVs that are displayed in panel c in the Niskin and underway seawater samples.

in colony microbiomes were just two ASVs (Figure 6c). Both of these ASVs were also detected in seawater samples, but the ASV classified as *Profundimonas* sp. was enriched in colony microbiomes compared to in seawater samples (Figure 6c,d).

Geographical variation of ASVs found in single-colony microbiomes

The environmental bacterial communities were further interrogated to investigate how the relative abundance of bacterial ASVs that were found to be associated with field-collected *Phaeocystis* colonies changed in seawater samples as the relative abundance of *Phaeocystis* changed. Alteromonadales made dominated field-collected colony microbiomes, with the genera *Paraglaciecola* and *Colwellia* contributing the most sequencing reads (Figure 5, Figure S7). Linear models fit with the lm function from the R stats package demonstrated that the relative abundance of *Paraglaciecola* ASVs in seawater samples was significantly related to the relative abundance of *Phaeocystis* in both the Niskin ($R^2 = 0.77$, $p = 0.05$, $F = 10.13$ on 1 and 3 *df*) and underway samples ($R^2 = 0.52$, $p = 0.008$, $F = 11.15$ on 1 and 10 *df*; Figure 7a), but the *Colwellia* ASVs were generally low abundance in environmental samples and did not correlate to *Phaeocystis* abundance ($R^2 = 0.11$, $p = 0.59$, $F = 0.37$ on 1 and 3 *df*; Figure 7b). Twenty-eight Oceanospirillales ASVs were detected in field-collected colony microbiomes, with two of these prominently prevalent and abundant across field-collected colony microbiomes (Figure S9). Of the 28 colony-associated Oceanospirillales ASVs, nine were also detected in the environmental samples, including the two that were most abundant in colony microbiomes, with the majority belonging to the Oceanospirillales family Nitrincolaceae (Figure 6). Linear models showed that the summed relative abundances of Nitrincolacea ASVs that were detected in both field-collected colony microbiomes and seawater samples were significantly related to the relative abundance of *Phaeocystis* in Niskin ($R^2 = 0.87$, $p = 0.02$, $F = 20.05$ on 1 and 3 *df*) and underway samples ($R^2 = 0.60$, $p = 0.003$, $F = 15.0$ on 1 and 10 *df*; Figure 7c). Sphingomonadales was the third most abundant order in field-collected colony microbiomes (Figure 4b), but Sphingomonadales ASVs were not detected in most environmental samples (max. rel. abundance in any sample = 0.04%), and the Sphingomonadales ASVs

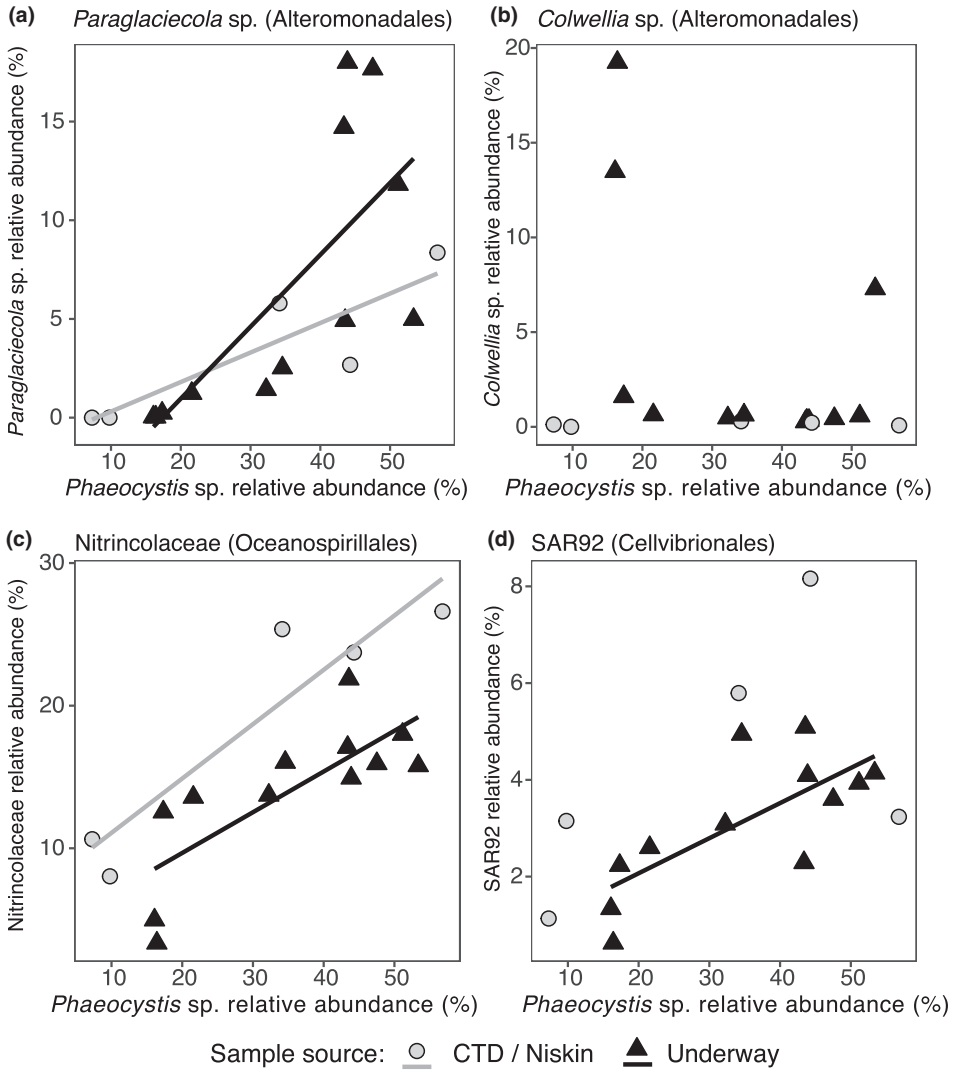

FIGURE 7 Linear regression between the relative abundance of *Phaeocystis* chloroplast 16S ASVs and the relative abundance of 16S rRNA gene sequences of key bacterial groups in each seawater sample. *Phaeocystis* amplicon sequence variants (ASV) relative abundance is on the *x*-axis of all panels. *Paraglaciecola* sp. ASV relative abundance is summed and plotted on the *y*-axis in panel a (Niskin $R^2 = 0.77$, $p = 0.05$; underway $R^2 = 0.52$, $p = 0.008$); *Colwellia* sp. ASV relative abundance is summed and plotted on the *y*-axis in panel b (Niskin $p > 0.05$; underway $p > 0.05$.); Nitrinocolaceae ASV relative abundance is summed and plotted on the *y*-axis in panel c (Niskin $R^2 = 0.87$, $p = 0.02$; underway $R^2 = 0.36$, $p = 0.04$); and SAR92 ASV relative abundance is plotted on the *y*-axis in panel d (Niskin samples $p > 0.05$; underway $R^2 = 0.54$, $p = 0.006$). Regression lines are only shown when linear model results were statistically significant ($p < 0.05$). For this analysis, ASVs in seawater were subset to only include ASVs that were also in field-collected colony microbiomes.

in colony microbiomes were not detected in any environmental samples. Cellvibrionales, which includes the SAR92 clade whose abundance was previously reported to be strongly associated with *Phaeocystis* biomass (Delmont et al., 2014), was the next most abundant order in the field-collected colony microbiomes. Thus, we directly compared SAR92 ASV relative abundance to *Phaeocystis* relative abundance in our samples with a linear regression and determined the relative abundance of the two groups to be significantly related in underway samples ($R^2 = 0.54$, $p = 0.006$, $F = 11.85$ on 1 and 10 *df*) but not in Niskin samples ($R^2 = 0.30$, $p = 0.34$, $F = 1.27$ on 1 and 3 *df*).

DISCUSSION

By directly evaluating microbiomes of *Phaeocystis antarctica* colonies from the field, we demonstrated that *P. antarctica* colonies host consistent microbiomes even when sampled from geographically distinct locations (~108 nautical miles apart) within a single season. This result is consistent with previous work showing that *P. globosa* colonies hosted similar microbiome communities regardless of from where the culture originated (Mars Brisbin et al., 2022). However, when *P. antarctica* was cultured and maintained in a walk-in cold chamber with 24-h fluorescent lighting for 1 year, the microbiome

diversity was halved, and the overall composition shifted from being mainly composed of Alteromonadales, Oceanospirillales, and Sphingomonadales to being dominated by Caulobacterales, Cellvibrionales, and Rhodobacterales (Figure 2). The dominant constituent of field-collected *P. antarctica* colony microbiomes was *Paraglaciecola* sp. (Alteromonadales), a psychrophile previously observed in association with sea ice and ice algae (Vadillo Gonzalez et al., 2022). The second most prevalent field-collected colony microbiome constituent, *Colwellia* sp., is also psychrophilic (Methé et al., 2005; Zhang et al., 2017). Similarly, a prevalent Oceanospirillales ASV (genus: *Profundimonas*) in field-collected colony microbiomes has been predicted to be psychrophilic (Cao et al., 2014). These psychrophiles were lost or reduced in culture, probably due to temperature variation during transport and incubation at ~4°C instead of –1°C, which was the surface seawater temperature when colonies were collected. However, the precise loss point or cause cannot be definitively identified because the cultured colony microbiome was only evaluated at the end of the culture period. Moreover, cultures represented altered nutrient and light regimes that could have further influenced the co-cultured bacterial community structure. Rhodobacterales—a group often reported to associate with phytoplankton phycospheres (Beiralas et al., 2023; Roager et al., 2024)—became a dominant contributor to cultured colony microbiomes, suggesting that this group may be well suited to laboratory conditions typical of phytoplankton culture and, therefore, may increase in relative abundance during culture. These results highlight the importance of investigating microbial interactions in situ, especially when environmental conditions are difficult to reproduce, as is true of polar environments.

To assess the significance of *Phaeocystis antarctica*-associated bacteria in a broader environmental context, the relative abundances of ASVs belonging to major colony-associated taxonomic groups (Alteromonadales, Oceanospirillales, Sphingomonadales) were compared to the relative abundance of ASVs classified as *Phaeocystis* chloroplast in each seawater sample. *Paraglaciecola* (Alteromonadales) relative abundance was correlated to *Phaeocystis* abundance, demonstrating that this dominant microbiome constituent was more abundant in surface seawater when *Phaeocystis* was more abundant (Figure 3). *Paraglaciecola* spp. are motile (Wang et al., 2020), particle-associated marine bacteria (Heins et al., 2021) with a diverse array of functional carbohydrate-active enzymes (CAZymes) that allow them to metabolize algae-specific complex polysaccharides, including agars, carrageenans, alginates, and fucoidans (Schultz-Johansen et al., 2018). Therefore, *Paraglaciecola* may be particularly suited to actively colonize *P. antarctica* colonies and utilize the abundant and diverse polysaccharides that comprise the *P. antarctica* colonial matrix and are excreted by *P. antarctica* cells (Alderkamp et al., 2007). Similar to *Paraglaciecola* ASVs, Oceanospirillales ASVs (family: Nitrincolaceae) detected in the field-collected colony microbiomes were more abundant in surface seawater samples when *Phaeocystis* was also more abundant (Figure 7). Although less is known about their metabolic capabilities, the abundance of Nitrincolacea has been correlated to phytoplankton biomass in polar waters (Liu et al., 2020; Thiele et al., 2023; Wietz et al., 2021), and Nitrincolacea are often first responders to increasing organic carbon availability at the start of phytoplankton blooms (Liu et al., 2020; Thiele et al., 2023).

In contrast to *Paraglaciecola* and Nitrincolaecea, *Colwellia* spp. (Alteromonadales) relative abundance was generally lower in surface water samples and uncorrelated with *Phaeocystis* abundance, despite being relatively abundant in all field-collected colony microbiomes (Figure 3). A previous study comparing bacterial communities inside and outside Southern Ocean *Phaeocystis* blooms determined *Colwellia* abundance correlated with *Phaeocystis* abundance at depth but not at the surface, leading the authors to hypothesize that *Colwellia* was active in degrading sinking *Phaeocystis* colony biomass (Delmont et al., 2014). Corroborating this hypothesis, another study observed that *Colwellia* spp. were initially rare within bacterial communities on sinking particles collected in the Arctic but became abundant after a 10-day incubation (Heins et al., 2021). In our present study, *Colwellia* was determined to be prevalent across field-collected colony microbiomes by assessing the 16S rRNA gene (DNA), whereas the environmental communities in surface seawater were assessed with 16S rRNA (RNA), and *Colwellia* was barely detected in most of these samples. Sequences originating from RNA instead of DNA provide insight into activity in addition to abundance (Li et al., 2017), suggesting that the *Colwellia* in colony microbiomes could be relatively inactive. Colony-associated *Colwellia* may become more active in response to senescence-associated changes in the *Phaeocystis* colony microhabitat as *Phaeocystis* sinks and senesces at depth. Although additional sampling would be necessary to directly test this, phycosphere-associated bacteria have been shown to respond metabolically to algal senescence (Seyedsayamdost et al., 2011). *Colwellia* could also become more active and abundant in surface waters later in the season as the *Phaeocystis* bloom declines and colonies senesce before sinking. Ultimately, time-course single-colony, surface-water, and subsurface-water samples collected from the beginning of the bloom through bloom demise would be needed to fully evaluate the role of *Colwellia* in degrading *Phaeocystis* colony biomass.

SAR92 (Order: Cellvibrionales) was previously reported as the bacterial group most strongly correlated with *Phaeocystis* abundance in surface waters and was also determined to be enriched in the particulate

size fraction during *P. antarctica* blooms (Delmont et al., 2014). A SAR92 ASV contributed 0%–18% (mean = 2.8%) of bacterial 16S rRNA gene sequences generated for field-collected colony microbiomes (absent in cultured colony microbiomes), confirming this previously hypothesized association. The SAR92 ASV ranged in relative abundance from 0.6% to 8.2% (mean = 3.5%) in our surface water samples, which was lower than the 30%–40% of sequences from >3 μm samples reported in Delmont et al. (2014). The SAR92 ASV was significantly correlated with *Phaeocystis* abundance in our underway samples ($R^2 = 0.54$, $p = 0.006$)—which excluded the 0.2–3-μm-size fraction—but not the CTD samples ($R^2 = 0.3$, $p = 0.34$) that were unfractionated. SAR92 relative abundance increases during phytoplankton blooms, especially at high latitudes, suggesting it may generally respond to phytoplankton biomass and phytoplankton-derived organic matter (Liu et al., 2020; Teeling et al., 2016; Wemheuer et al., 2015; Xue et al., 2021). However, SAR92 can use dimethylsulfoniopropionate (DMSP) as its sole carbon source by enzymatically cleaving DMSP and releasing climatically active dimethyl sulfide (DMS; He et al., 2023). When experimentally exposed to elevated DMSP, SAR92 upregulated expression of the DMSP cleavage pathway, demonstrating that DMSP is an important carbon source for these bacteria (He et al., 2023). As *Phaeocystis* is a prolific producer of DMSP (DiTullio et al., 2000; van Duyl et al., 1998; Vance et al., 2013), SAR92 may be especially poised to respond to *Phaeocystis* blooms and associate with *Phaeocystis* colonies. Moreover, the physical coupling of SAR92 bacteria and *P. antarctica* colonies may expedite DMS production and release to the atmosphere, influencing cloud formation, atmospheric processes, and climate feedbacks (Park et al., 2021).

Phytoplankton–bacteria interactions have the potential to drive bloom formation, decline, and succession, with consequences for the food web and carbon sequestration (Cirri & Pohnert, 2019; Seymour et al., 2017). *Phaeocystis* is an important contributor to primary production and carbon export in the Southern Ocean, but many aspects of its physiology—particularly drivers of its blooms—remain enigmatic. We showed that *P. antarctica* colonies had consistent microbiomes when collected from two sites in the Palmer LTER grid. Most of the dominant field-collected colony-associated bacteria can move toward regions of interest, colonize particles, and metabolize polysaccharides and nitrogen compounds that are relatively unique to the *Phaeocystis* colonial matrix. Thus, bacteria associated with colonies likely benefit from the association through chemical currencies made available by *Phaeocystis* cells. However, it remains unclear as to how or if *Phaeocystis* benefits from hosting these specific microbiome communities. *Paraglaciecola* followed by *Colwellia* were the most prevalent microbiome constituents for field-collected colonies. All of the completed *Paraglaciecola* ($n = 3$) and *Colwellia* ($n = 7$) genomes that are annotated in the KEGG database (Kanehisa et al., 2023) have complete salvage and repair pathways for building vitamin B_{12} from precursor cobamides (Fang et al., 2017; Rodionov et al., 2003). A marine *Colwellia* isolate was shown to require B_{12} for growth and was rescued from B_{12} limitation if cobamides were supplied. Moreover, when *Colwellia* was grown on cobamides, it shared B_{12} with two different B_{12}-requiring diatoms, rescuing them from B_{12} limitation in experimental conditions. The *Colwellia* also released another B_{12} precursor, the lower ligand α-ribazole that could be used by other bacteria to build B_{12} (Wienhausen et al., 2024). Thus, it is conceivable that microbiome bacteria, either individually or in concert, provide *P. antarctica* with B_{12}, a service that is common among phytoplankton microbiomes (e.g., Cruz-López & Maske, 2016; Durham et al., 2015) and that would give *P. antarctica* a competitive boost at the start of the spring bloom (Bertrand et al., 2007; Joy-Warren et al., 2022). Given that this study emphasizes the importance of studying microbial interactions in situ and cautions against evaluating microbial interactions in culture conditions (especially for polar species), culture experiments investigating the roles of *P. antarctica* colony microbiomes may not be representative. Instead, the direct sequencing of *Phaeocystis*—and other phytoplankton—microbiomes provides a road map for which bacteria to target in meta-omic analyses. For instance, future work may target the transcriptional activity of *Paraglaciecola* in the particulate size fraction of seawater samples from a *Phaeocystis* bloom to elucidate benefits bestowed by colony microbiomes.

The WAP region is undergoing rapid environmental change, with air and sea surface temperatures having increased ~6°C and 1°C, respectively, since the mid-1900s (Meredith & King, 2005). Warming has caused glacial retreat (Cook et al., 2016) and reduced sea ice coverage and annual sea ice duration in the region (Stammerjohn et al., 2021). With phytoplankton community composition and bloom biomass tightly coupled to seasonal sea ice retreat and its impact on mix layer depth and nutrient availability, ongoing shifts in dominant phytoplankton bloom taxa (Nardelli et al., 2023) and phenology (i.e., timing of annual bloom events) are expected to continue (Turner et al., 2024). Although the overall spring bloom onset is shifting to later in the year, the bloom in the offshore region—where *Phaeocystis antarctica* is more likely to be abundant (Joy-Warren et al., 2019)—is occurring slightly earlier (Turner et al., 2024). Increasing temperature and changing environmental conditions associated with altered bloom timing are likely to influence phytoplankton microbiome composition and function, especially if major microbiome constituents are psychrophilic. As

environmental conditions continue to shift with global climate change, it will be increasingly important to comprehensively characterize interactions between phytoplankton and their microbiomes and determine how changes to these relationships may propagate through the ecosystem.

AUTHOR CONTRIBUTIONS

Margaret Mars Brisbin: Conceptualization (lead); data curation (lead); formal analysis (lead); funding acquisition (supporting); investigation (lead); methodology (lead); project administration (lead); visualization (lead); writing – original draft (lead); writing – review and editing (lead). **McCaela Acord:** Investigation (supporting); methodology (supporting); writing – review and editing (equal). **Rachel Davitt:** Investigation (supporting); methodology (supporting); writing – review and editing (equal). **Shavonna Bent:** Investigation (supporting); methodology (supporting); writing – review and editing (equal). **Benjamin A. S. Van Mooy:** Funding acquisition (lead); methodology (supporting); project administration (lead); resources (supporting); writing – review and editing (equal). **Eliott Flaum:** Data curation (supporting); investigation (supporting); methodology (supporting); visualization (supporting); writing – review and editing (equal). **Andreas Norlin:** Writing – review and editing (equal). **Jessica Turner:** Data curation (supporting); formal analysis (supporting); investigation (supporting); methodology (supporting); visualization (supporting); writing – review and editing (equal). **Arianna Krinos:** Visualization (supporting); writing – review and editing (equal). **Harriet Alexander:** Conceptualization (supporting); funding acquisition (supporting); project administration (supporting); resources (supporting); supervision (supporting); writing – review and editing (equal). **Mak Saito:** Conceptualization (supporting); funding acquisition (supporting); project administration (supporting); resources (supporting); supervision (supporting); writing – review and editing (equal).

ACKNOWLEDGMENTS

We thank the captain and crew of the R/V Nathaniel B. Palmer along with the scientists and scientific support staff associated with the PAL LTER program for their assistance in sample collection and underway measurements. This work was supported by National Science Foundation OPP-2224611 to BASVM. MMB was supported by the Simons Foundation through a Marine Microbial Ecology Postdoctoral Fellowship (award 874439). MA was supported through the Blue Economy Internship program at WHOI, which is supported in part by John and Shirley Farrington. We further thank Gretta Serres, Julie Huber, and Kama Thieler for their leadership roles in the Blue Economy Internship program. Sequencing for this project was completed by the Georgia Genomics and Bioinformatics Core (GGBC, UG Athens, GA, RRID: SCR_010994).

DATA AVAILABILITY STATEMENT

All sequencing data generated for this project are available from the NCBI SRA under accession PRJNA1136990. Intermediate data files and the code necessary to replicate the analyses are available in a GitHub repository (https://github.com/MICOlab-USF/phaeosphere_AntarcticEdition) and as an interactive HTML document (https://micolab-usf.github.io/phaeosphere_AntarcticEdition/Phaeosphere_Analysis.html).

ORCID

Margaret Mars Brisbin https://orcid.org/0000-0001-7756-0039

REFERENCES

Alderkamp, A.-C., Buma, A. G. J., & van Rijssel, M. (2007). The carbohydrates of *Phaeocystis* and their degradation in the microbial food web. *Biogeochemistry*, *83*, 99–118.

Andrew, S., Wilson, T., Smith, S., Marchetti, A., & Septer, A. N. (2022). A tripartite model system for Southern Ocean diatom-bacterial interactions reveals the coexistence of competing symbiotic strategies. *ISME Communications*, *2*, 97.

Arrigo, K. R., Worthen, D., Schnell, A., & Lizotte, M. P. (1998). Primary production in Southern Ocean waters. *Journal of Geophysical Research*, *103*, 15587–15600.

Beiralas, R., Ozer, N., & Segev, E. (2023). Abundant *Sulfitobacter* marine bacteria protect *Emiliania huxleyi* algae from pathogenic bacteria. *ISME Communications*, *3*, 100.

Bertrand, E. M., McCrow, J. P., Moustafa, A., Zheng, H., McQuaid, J. B., Delmont, T. O., Post, A. F., Sipler, R. E., Spackeen, J. L., Xu, K., Bronk, D. A., Hutchins, D. A., & Allen, A. E. (2015). Phytoplankton-bacterial interactions mediate micronutrient colimitation at the coastal Antarctic sea ice edge. *Proceedings of the National Academy of Sciences of the United States of America*, *112*, 9938–9943.

Bertrand, E. M., Saito, M. A., Rose, J. M., Riesselman, C. R., Lohan, M. C., Noble, A. E., Lee, P. A., & DiTullio, G. R. (2007). Vitamin B_{12} and iron colimitation of phytoplankton growth in the Ross Sea. *Limnology and Oceanography*, *52*, 1079–1093.

Bokulich, N. A., Kaehler, B. D., Rideout, J. R., Dillon, M., Bolyen, E., Knight, R., Huttley, G. A., & Gregory Caporaso, J. (2018). Optimizing taxonomic classification of marker-gene amplicon sequences with QIIME 2's q2-feature-classifier plugin. *Microbiome*, *6*, 90.

Bolyen, E., Rideout, J. R., Dillon, M. R., Bokulich, N. A., Abnet, C. C., Al-Ghalith, G. A., Alexander, H., Alm, E. J., Arumugam, M., Asnicar, F., Bai, Y., Bisanz, J. E., Bittinger, K., Brejnrod, A., Brislawn, C. J., Brown, C. T., Callahan, B. J., Caraballo-Rodríguez, A. M., Chase, J., … Caporaso, J. G. (2019). Reproducible, interactive, scalable and extensible microbiome data science using QIIME 2. *Nature Biotechnology*, *37*, 852–857.

Brown, M. S., Munro, D. R., Feehan, C. J., Sweeney, C., Ducklow, H. W., & Schofield, O. M. (2019). Enhanced oceanic CO_2 uptake along the rapidly changing West Antarctic Peninsula. *Nature Climate Change*, *9*, 678–683.

Callahan, B. J., McMurdie, P. J., Rosen, M. J., Han, A. W., Johnson, A. J. A., & Holmes, S. P. (2016). DADA2: High-resolution sample inference from Illumina amplicon data. *Nature Methods*, *13*, 581–583.

Cao, Y., Chastain, R. A., Eloe, E. A., Nogi, Y., Kato, C., & Bartlett, D. H. (2014). Novel psychropiezophilic Oceanospirillales species *Profundimonas piezophila* gen. nov., sp. nov., isolated from the deep-sea environment of the Puerto Rico trench. *Applied and Environmental Microbiology*, *80*, 54–60.

Cirri, E., & Pohnert, G. (2019). Algae–bacteria interactions that balance the planktonic microbiome. *The New Phytologist*, *223*, 100–106.

Cook, A. J., Holland, P. R., Meredith, M. P., Murray, T., Luckman, A., & Vaughan, D. G. (2016). Ocean forcing of glacier retreat in the western Antarctic Peninsula. *Science*, *353*, 283–286.

Cruz-López, R., & Maske, H. (2016). The vitamin B1 and B12 required by the marine dinoflagellate *Lingulodinium polyedrum* can be provided by its associated bacterial community in culture. *Frontiers in Microbiology*, *7*, 560.

Decelle, J., Romac, S., Stern, R. F., Bendif, E. M., Zingone, A., Audic, S., Guiry, M. D., Guillou, L., Tessier, D., le Gall, F., Gourvil, P., dos Santos, A. L., Probert, I., Vaulot, D., de Vargas, C., & Christen, R. (2015). PhytoREF: A reference database of the plastidial 16S rRNA gene of photosynthetic eukaryotes with curated taxonomy. *Molecular Ecology Resources*, *15*, 1435–1445.

Delmont, T. O., Hammar, K. M., Ducklow, H. W., Yager, P. L., & Post, A. F. (2014). *Phaeocystis antarctica* blooms strongly influence bacterial community structures in the Amundsen Sea polynya. *Frontiers in Microbiology*, *5*, 646.

DiTullio, G. R., Grebmeier, J. M., Arrigo, K. R., Lizotte, M. P., Robinson, D. H., Leventer, A., Barry, J. P., VanWoert, M. L., & Dunbar, R. B. (2000). Rapid and early export of *Phaeocystis antarctica* blooms in the Ross Sea, Antarctica. *Nature*, *404*, 595–598.

Durham, B. P., Sharma, S., Luo, H., Smith, C. B., Amin, S. A., Bender, S. J., Dearth, S. P., van Mooy, B. A. S., Campagna, S. R., Kujawinski, E. B., Armbrust, E. V., & Moran, M. A. (2015). Cryptic carbon and sulfur cycling between surface ocean plankton. *Proceedings of the National Academy of Sciences of the United States of America*, *112*, 453–457.

Fang, H., Kang, J., & Zhang, D. (2017). Microbial production of vitamin B_{12}: A review and future perspectives. *Microbial Cell Factories*, *16*, 15.

Friedman, J., & Alm, E. J. (2012). Inferring correlation networks from genomic survey data. *PLoS Computational Biology*, *8*, e1002687.

Garnesson, P., Mangin, A., Fanton d'Andon, O., Demaria, J., & Bretagnon, M. (2019). The CMEMS GlobColour chlorophyll *a* product based on satellite observation: Multi-sensor merging and flagging strategies. *Ocean Science*, *15*, 819–830.

Gloor, G. B., Macklaim, J. M., Pawlowsky-Glahn, V., & Egozcue, J. J. (2017). Microbiome datasets are compositional: And this is not optional. *Frontiers in Microbiology*, *8*, 2224.

Guillard, R. R. L., & Hargraves, P. E. (1993). *Stichochrysis immobilis* is a diatom, not a chrysophyte. *Phycologia*, *32*, 234–236.

He, X.-Y., Liu, N.-H., Liu, J.-Q., Peng, M., Teng, Z.-J., Gu, T.-J., Chen, X.-L., Chen, Y., Wang, P., Li, C. Y., Todd, J. D., Zhang, Y. Z., & Zhang, X. Y. (2023). SAR92 clade bacteria are potentially important DMSP degraders and sources of climate-active gases in marine environments. *MBio*, *14*, e0146723.

Heins, A., Amann, R. I., & Harder, J. (2021). Cultivation of particle-associated heterotrophic bacteria during a spring phytoplankton bloom in the North Sea. *Systematic and Applied Microbiology*, *44*, 126232.

Joy-Warren, H. L., Alderkamp, A.-C., Dijken, G. L., Jabre, L., Bertrand, E. M., Baldonado, E. N., Glickman, M. W., Lewis, K. M., Middag, R., Seyitmuhammedov, K., Lowry, K. E., van de Poll, W., & Arrigo, K. R. (2022). Springtime phytoplankton responses to light and iron availability along the western Antarctic Peninsula. *Limnology and Oceanography*, *67*, 800–815.

Joy-Warren, H. L., van Dijken, G. L., Alderkamp, A.-C., Leventer, A., Lewis, K. M., Selz, V., Lowry, K. E., van de Poll, W., & Arrigo, K. R. (2019). Light is the primary driver of early season phytoplankton production along the western Antarctic Peninsula. *Journal of Geophysical Research, C: Oceans*, *124*, 7375–7399.

Kanehisa, M., Furumichi, M., Sato, Y., Kawashima, M., & Ishiguro-Watanabe, M. (2023). KEGG for taxonomy-based analysis of pathways and genomes. *Nucleic Acids Research*, *51*, D587–D592.

Kim, H. H., Bowman, J. S., Luo, Y.-W., Ducklow, H. W., Schofield, O. M., Steinberg, D. K., & Doney, S. C. (2022). Modeling polar marine ecosystem functions guided by bacterial physiological and taxonomic traits. *Biogeosciences*, *19*, 117–136.

Kim, H. H., Laufkötter, C., Lovato, T., Doney, S. C., & Ducklow, H. W. (2023). Projected 21st-century changes in marine heterotrophic bacteria under climate change. *Frontiers in Microbiology*, *14*, 1049579.

Klindworth, A., Pruesse, E., Schweer, T., Peplies, J., Quast, C., Horn, M., & Glöckner, F. O. (2013). Evaluation of general 16S ribosomal RNA gene PCR primers for classical and next-generation sequencing-based diversity studies. *Nucleic Acids Research*, *41*, e1.

Kuhlisch, C., Shemi, A., Barak-Gavish, N., Schatz, D., & Vardi, A. (2024). Algal blooms in the ocean: Hot spots for chemically mediated microbial interactions. *Nature Reviews Microbiology*, *22*, 138–154.

Li, R., Tun, H. M., Jahan, M., Zhang, Z., Kumar, A., Dilantha Fernando, W. G., Farenhorst, A., & Khafipour, E. (2017). Comparison of DNA-, PMA-, and RNA-based 16S rRNA Illumina sequencing for detection of live bacteria in water. *Scientific Reports*, *7*, 5752.

Liu, Y., Blain, S., Crispi, O., Rembauville, M., & Obernosterer, I. (2020). Seasonal dynamics of prokaryotes and their associations with diatoms in the Southern Ocean as revealed by an autonomous sampler. *Environmental Microbiology*, *22*, 3968–3984.

Mars Brisbin, M., Mitarai, S., Saito, M. A., & Alexander, H. (2022). Microbiomes of bloom-forming *Phaeocystis* algae are stable and consistently recruited, with both symbiotic and opportunistic modes. *The ISME Journal*, *16*, 2255–2264.

Martínez-Pérez, C., Zweifel, S. T., Pioli, R., & Stocker, R. (2024). Space, the final frontier: The spatial component of phytoplankton-bacterial interactions. *Molecular Microbiology*, *122*, 331–346.

McMurdie, P. J., & Holmes, S. (2013). phyloseq: An R package for reproducible interactive analysis and graphics of microbiome census data. *PLoS ONE*, *8*, e61217.

Meredith, M. P., & King, J. C. (2005). Rapid climate change in the ocean west of the Antarctic Peninsula during the second half of the 20th century. *Geophysical Research Letters*, *32*, L19604.

Methé, B. A., Nelson, K. E., Deming, J. W., Momen, B., Melamud, E., Zhang, X., Moult, J., Madupu, R., Nelson, W. C., Dodson, R. J., Brinkac, L. M., Daugherty, S. C., Durkin, A. S., DeBoy, R. T., Kolonay, J. F., Sullivan, S. A., Zhou, L., Davidsen, T. M., Wu, M., … Fraser, C. M. (2005). The psychrophilic lifestyle as revealed by the genome sequence of *Colwellia psychrerythraea* 34H through genomic and proteomic analyses. *Proceedings of the National Academy of Sciences of the United States of America*, *102*, 10913–10918.

Nardelli, S. C., Gray, P. C., Stammerjohn, S. E., & Schofield, O. (2023). Characterizing coastal phytoplankton seasonal succession patterns on the West Antarctic Peninsula. *Limnology and Oceanography*, *68*, 845–861.

Nissen, C., & Vogt, M. (2021). Factors controlling the competition between *Phaeocystis* and diatoms in the Southern Ocean and implications for carbon export fluxes. *Biogeosciences*, *18*, 251–283.

Oksanen, J., Simpson, G., Blanchet, F., Kindt, R., Legendre, P., Minchin, P., O'Hara, R., Solymos, P., Stevens, M., Szoecs, E., Wagner, H., Barbour, M., Bedward, M., Bolker, B., Borcard, D.,

Borman, T., Carvalho, G., Chirico, M., De Caceres, M., … Weedon, J. (2025). vegan: Community ecology package. R package version 2.8-0. https://vegandevs.github.io/vegan/

Park, K.-T., Yoon, Y. J., Lee, K., Tunved, P., Krejci, R., Ström, J., Jang, E., Park, K.-. T., Kang, H. J., Jang, S., Park, J., Lee, B. Y., Traversi, R., Becagli, S., & Hermansen, O. (2021). Dimethyl sulfide-induced increase in cloud condensation nuclei in the Arctic atmosphere. *Global Biogeochemical Cycles*, *35*, e2021GB006969.

Quast, C., Pruesse, E., Yilmaz, P., Gerken, J., Schweer, T., Yarza, P., Peplies, J., & Glöckner, F. O. (2013). The SILVA ribosomal RNA gene database project: Improved data processing and web-based tools. *Nucleic Acids Research*, *41*, D590–D596.

R Core Team. (2018). *R: A language and environment for statistical computing*. R Foundation for Statistical Computing.

Roager, L., Kempen, P. J., Bentzon-Tilia, M., Sonnenschein, E. C., & Gram, L. (2024). Impact of host species on assembly, composition, and functional profiles of phycosphere microbiomes. *mSystems*, *9*, e0058324.

Rodionov, D. A., Vitreschak, A. G., Mironov, A. A., & Gelfand, M. S. (2003). Comparative genomics of the vitamin B_{12} metabolism and regulation in prokaryotes. *The Journal of Biological Chemistry*, *278*, 41148–41159.

Ryderheim, F., Hansen, P. J., & Kiørboe, T. (2022). Predator field and colony morphology determine the defensive benefit of colony formation in marine phytoplankton. *Frontiers in Marine Science*, *9*, 829419.

Schoemann, V., Becquevort, S., Stefels, J., Rousseau, V., & Lancelot, C. (2005). *Phaeocystis* blooms in the global ocean and their controlling mechanisms: A review. *Journal of Sea Research*, *53*, 43–66.

Schofield, O., Ducklow, H. W., Martinson, D. G., Meredith, M. P., Moline, M. A., & Fraser, W. R. (2010). How do polar marine ecosystems respond to rapid climate change? *Science*, *328*, 1520–1523.

Schofield, O., Saba, G., Coleman, K., Carvalho, F., Couto, N., Ducklow, H., Finkel, Z., Irwin, A., Kahl, A., Miles, T., Montes-Hugo, M., Stammerjohn, S., & Waite, N. (2017). Decadal variability in coastal phytoplankton community composition in a changing West Antarctic Peninsula. *Deep Sea Research Part I: Oceanographic Research Papers*, *124*, 42–54.

Schultz-Johansen, M., Bech, P. K., Hennessy, R. C., Glaring, M. A., Barbeyron, T., Czjzek, M., & Stougaard, P. (2018). A novel enzyme portfolio for red algal polysaccharide degradation in the marine bacterium *Paraglaciecola hydrolytica* S66T encoded in a sizeable polysaccharide utilization locus. *Frontiers in Microbiology*, *9*, 839.

Seyedsayamdost, M. R., Case, R. J., Kolter, R., & Clardy, J. (2011). The Jekyll-and-Hyde chemistry of *Phaeobacter gallaeciensis*. *Nature Chemistry*, *3*, 331–335.

Seymour, J. R., Amin, S. A., Raina, J.-B., & Stocker, R. (2017). Zooming in on the phycosphere: The ecological interface for phytoplankton-bacteria relationships. *Nature Microbiology*, *2*, 17065.

Smith, W. O., Jr., & Trimborn, S. (2024). *Phaeocystis*: A global enigma. *Annual Review of Marine Science*, *16*, 417–441.

Smith, W. O., Jr., Zhang, W. G., Hirzel, A., Stanley, R. M., Meyer, M. G., Sosik, H., Alatalo, P., Oliver, H., Sandwith, Z., Crockford, E. T., Peacock, E. E., Mehta, A., & McGillicuddy, D. J., Jr. (2021). A regional, early spring bloom of *Phaeocystis pouchetii* on the New England continental shelf. *Journal of Geophysical Research: Oceans*, *126*, e2020JC016856. https://doi.org/10.1029/2020JC016856

Stammerjohn, S., Massom, R., Rind, D., & Martinson, D. (2021). Regions of rapid sea ice change: An inter-hemispheric seasonal comparison. *Geophysical Research Letters*, *39*, L06501.

Teeling, H., Fuchs, B. M., Bennke, C. M., Krüger, K., Chafee, M., Kappelmann, L., Reintjes, G., Waldmann, J., Quast, C., Glöckner, F. O., Lucas, J., Wichels, A., Gerdts, G., Wiltshire, K. H., & Amann, R. I. (2016). Recurring patterns in bacterioplankton dynamics during coastal spring algae blooms. *eLife*, *5*, e11888.

Thiele, S., Vader, A., Thomson, S., Saubrekka, K., Petelenz, E., Müller, O., Bratbak, G., & Øvreås, L. (2023). Seasonality of the bacterial and archaeal community composition of the Northern Barents Sea. *Frontiers in Microbiology*, *14*, 1213718.

Turner, J. S., Dierssen, H., Schofield, O., Kim, H. H., Stammerjohn, S., Munro, D. R., & Kavanaugh, M. (2024). Changing phytoplankton phenology in the marginal ice zone west of the Antarctic Peninsula. *Marine Ecology Progress Series*, *734*, 1–21. https://doi.org/10.3354/meps14567

Vadillo Gonzalez, S., Clark, G. F., Johnston, E. L., Turney, C. S. M., Fogwill, C. J., Steinberg, P. D., & Marzinelli, E. M. (2022). Spatial variation in microbial communities associated with sea-ice algae in Commonwealth Bay, East Antarctica. *Microbiology*, *168*, 001176.

van Duyl, F. C., Gieskes, W. W. C., Kop, A. J., & Lewis, W. E. (1998). Biological control of short-term variations in the concentration of DMSP and DMS during a *Phaeocystis* spring bloom. *Journal of Sea Research*, *40*, 221–231.

Vance, T. R., Davidson, A. T., Thomson, P. G., Levasseur, M., Lizotte, M., Curran, M. A. J., & Jones, G. B. (2013). Rapid DMSP production by an Antarctic phytoplankton community exposed to natural surface irradiances in late spring. *Aquatic Microbial Ecology*, *71*, 117–129.

Wang, Y., Zhang, Y., Liu, T., Zhu, X., Ma, J., Su, X., Kang, J., & Guo, C. (2020). *Paraglaciecola marina* sp. nov., isolated from marine alga (*Sargassum natans* (L.) Gaillon). *International Journal of Systematic and Evolutionary Microbiology*, *70*, 4451–4457.

Wemheuer, B., Wemheuer, F., Hollensteiner, J., Meyer, F.-D., Voget, S., & Daniel, R. (2015). The green impact: Bacterioplankton response toward a phytoplankton spring bloom in the southern North Sea assessed by comparative metagenomic and metatranscriptomic approaches. *Frontiers in Microbiology*, *6*, 805.

Wienhausen, G., Moraru, C., Bruns, S., Tran, D. Q., Sultana, S., Wilkes, H., Dlugosch, L., Azam, F., & Simon, M. (2024). Ligand cross-feeding resolves bacterial vitamin B12 auxotrophies. *Nature*, *629*, 886–892.

Wietz, M., Bienhold, C., Metfies, K., Torres-Valdés, S., von Appen, W.-J., Salter, I., & Boetius, A. (2021). The polar night shift: Seasonal dynamics and drivers of Arctic Ocean microbiomes revealed by autonomous sampling. *ISME Communications*, *1*, 76.

Xue, C., Xie, Z.-X., Li, Y.-Y., Chen, X.-H., Sun, G., Lin, L., Giovannoni, S. J., & Wang, D. Z. (2021). Polysaccharide utilization by a marine heterotrophic bacterium from the SAR92 clade. *FEMS Microbiology Ecology*, *97*, fiab120.

Zhang, C., Guo, W., Wang, Y., & Chen, X. (2017). *Colwellia beringensis* sp. nov., a psychrophilic bacterium isolated from the Bering Sea. *International Journal of Systematic and Evolutionary Microbiology*, *67*, 5102–5107.

SUPPORTING INFORMATION

Additional supporting information can be found online in the Supporting Information section at the end of this article.

Figure S1. Representative *Phaeocystis antarctica* colonies isolated from station 600.200 in the PAL LTER grid and processed for microbiome analysis. Scale bars are 100 μm and images were taken at 200× magnification during the final rinse before transfer to PCR tubes for DNA extraction.

Figure S2. Relative abundance of bacterial and chloroplast 16S rRNA sequences in all samples.

Bacterial and chloroplast sequences were split and analyzed separately. Single-colony samples had 52%–96% chloroplast sequences.

Figure S3. Rarefaction curves for bacterial and chloroplast sequences in single-colony and surface seawater samples. Rarefaction was performed with the R package phyloseq and results were plotted with the ggrare function. All samples reached species (amplicon sequence variants [ASV]) richness saturation within the total number of sequences generated for the sample.

Figure S4. Bacterial alpha diversity in surface seawater samples collected by Niskin bottles on a CTD rosette and from the underway seawater system (A) near the West Antarctic Peninsula (B). (A) Top panels show per sample observed amplicon sequence variant (ASV) richness in CTD/Niskin and underway samples, while bottom panels show per sample Shannon indices in CTD/Niskin and underway samples. (B) Sample map shows CTD stations (red points; 400.100, 400.200, 500.200, 600.200, and 600.100) and underway samples on three lines—400-line (18–22), 600–500 transect (11–13), and the 600-line (7–10)—relative to the West Antarctic Peninsula.

Figure S5. Chloroplast alpha diversity in surface seawater samples collected by Niskin bottles on a CTD rosette and from the underway seawater system (A) near the West Antarctic Peninsula (B). (A) Top panels show per sample observed amplicon sequence variant (ASV) richness in CTD/Niskin and underway samples, while bottom panels show per sample Shannon indices in CTD/Niskin and underway samples. (B) Sample map shows CTD stations (red points; 400.100, 400.200, 500.200, 600.200, and 600.100) and underway samples on three lines—400-line (18–22), 600–500 transect (11–13), and the 600-line (7–10)—relative to the West Antarctic Peninsula.

Figure S6. Principal coordinates analysis (PCoA) of Aitchison distances between bacterial communities associated with individual field-collected and cultured *Phaeocystis antarctica* colonies. Point shape represents PAL LTER grid station of origin (either directly collected from or used to start a culture) and point color represents sample type (field-collected or cultured). Two main clusters are visible: communities associated with field-collected colonies and communities associated with cultured colonies. These clusters separate along the primary axis (*x*-axis), which explains 54.7% of the variability. The secondary axis explains only 6.6% of the variability and while there is some spread among field-collected colony communities on this axis, there is no separation by station.

Figure S7. Relative abundance of Alteromonadales amplicon sequence variants (ASVs) in field-collected and cultured colony microbiomes. Alteromonadales was the most dominant bacterial group in field-collected colonies but made up a small proportion of the cultured colony microbiomes. A single *Paraglaciecola* sp. ASV made up a large proportion of all field-collected colony microbiomes. Similarly, three *Colwellia* sp. ASVs were abundant in all field-collected colony microbiomes but were absent in cultured colony microbiomes. *Marinobacter* and *Glaciecola* ASVs were the only Alteromonadales ASVs detected in cultured colony microbiomes.

Figure S8. Relative abundance of Rhodobacterales amplicon sequence variants (ASVs) in field-collected and cultured colony microbiomes. Rhodobacterales was the second most abundant group in cultured colony microbiomes, but made up a small proportion of the field-collected colony microbiomes. A single *Sulfitobacter* sp. ASV made up a large proportion of all cultured colony microbiomes.

Figure S9. Relative abundance of Oceanospirillales amplicon sequence variants (ASVs) in field-collected and cultured colony microbiomes. Alteromonadales was the second most dominant bacterial group in field-collected colonies, but made up a small proportion of the cultured colony microbiomes. Two ASVs comprised a large proportion of all field-collected colony microbiomes, with one belonging to the genus *Profundimonas* (family: Nitrincolaceae) and the other being most similar to sequences from uncultured bacteria in the family Nitrincolaceae. Both of these ASVs were absent in cultured colony microbiomes. Instead, a *Saccharospirillum* ASV was the sole prevalent Oceanospirillales ASV in cultured colony microbiomes. *Saccharospirillum* spp. have been isolated from algal sediments and mangrove and seagrass rhizospheres, and while they can survive at low temperatures (4°C), their optimum growth temperatures are higher (25°C) (Yang et al., 2020).

Table S1. Summary of sequencing results for all samples. In the description column (Desc.), values beginning with A (e.g., A2) are individual *Phaeocystis* colonies from the Southern Ocean, "FT" refers to flow-through (underway) seawater samples, "CTD" refers to seawater samples collected from Niskin bottles on the CTD rosette, and samples beginning with "col" (e.g., "col1") are individual *Phaeocystis* colonies isolated after 1 year of culture.

How to cite this article: Mars Brisbin, M., Acord, M., Davitt, R., Bent, S., Van Mooy, B. A. S., Flaum, E., Norlin, A., Turner, J., Krinos, A., Alexander, H., & Saito, M. (2025). Exploring the Phaeosphere: Characterizing the microbiomes of *Phaeocystis antarctica* colonies from the coastal Southern Ocean and laboratory culture. *Journal of Phycology*, *61*, 1124–1139. https://doi.org/10.1111/jpy.70051